

Rough sea estimation for phase-shift de-ghosting

Sergio Grion, Rob Telling and Seb Holland, Dolphin Geophysical*

Summary

This paper discusses rough-sea de-ghosting for variable-depth streamer data. The de-ghosting algorithm is based on phase-shift wavefield extrapolators between non-planar interfaces and requires the solution of a linear system of equations. Analysis of the posterior covariance matrix from this inversion problem provides insight on the effect of cable shape and sea surface on de-ghosting results. The sea-surface is estimated using a tomographic approach. Application of the discussed algorithms to sample shot gathers acquired offshore Australia in the presence of a 2m SWH (significant wave height) rough sea provides satisfactory results.

Introduction

The pressure wavefield recorded by a horizontal or slanted streamer in the presence of a calm sea surface can be directly de-ghosted in a spectral domain. Horizontal and slanted de-ghosting algorithms are therefore computationally efficient, and in case of mild variations this restrictive assumption on streamer shape can be accommodated for by optimizing the ghost model parameters in time-space windows (Wang et al. 2013; Masoomzadeh et al. 2013; Grion et al. 2015).

Recently, variable-depth (Riyanti et al. 2008; Poole 2013) and rough sea-surface (King and Poole 2015; Hardwick et al. 2015) de-ghosting emerged as feasible and useful broadband processing steps. When changes in sea surface or receiver depth occur over short spatial distances, the spatial Fourier transform of the recorded wavefield gives a distorted representation of its wavenumbers. In this situation, the up-going wavefield is the solution to a linear system of equations. The fundamental building blocks of these equations are phase-shift redatuming operators that relate wavefields at different non-horizontal datums within the water column, for a constant or depth-varying water velocity profile. We therefore refer to this algorithm as phase-shift de-ghosting (Grion et al., 2016).

Phase-shift de-ghosting and cable depth estimation

Pressure recorded along the streamer cable c at a certain temporal frequency f and spatial location $\mathbf{x} = [x, y, z]$ is composed of an up-going and a down-going part:

$$\mathbf{p}_c(\mathbf{x}) = \mathbf{u}_c(\mathbf{x}) + \mathbf{d}_c(\mathbf{x}). \quad (1)$$

The $\mathbf{u}_c(\mathbf{x})$ and $\mathbf{d}_c(\mathbf{x})$ terms can be expressed in terms of the unknown wavenumber constituents $\mathbf{k} = [k_x, k_y]$ of the

up-going wavefield at mean sea level \mathbf{u}_0 :

$$\mathbf{u}_c(\mathbf{x}) = \mathbf{W}_{0c}^- \mathbf{u}_0(\mathbf{k}) \quad (2)$$

$$\mathbf{d}_c(\mathbf{x}) = r \mathbf{W}_{sc}^+ \mathbf{W}_{0s}^- \mathbf{u}_0(\mathbf{k}) \quad (3)$$

where \mathbf{W}_{0c}^- is the joint re-datuming and spatial reverse transform operator from mean sea level to cable, \mathbf{W}_{0s}^- and \mathbf{W}_{sc}^+ are the re-datuming operators from mean sea level to rough sea-surface and from rough sea-surface to streamer cable, respectively. The sea-surface reflectivity is r . In the \mathbf{W} notation, a '+' refers to the re-datuming of the down-going wavefield while a '-' is for the up-going. Substitution of (2) and (3) into (1) gives

$$\mathbf{p}_c(\mathbf{x}) = [\mathbf{W}_{0c}^- + r \mathbf{W}_{sc}^+ \mathbf{W}_{0s}^-] \mathbf{u}_0(\mathbf{k}) = \mathbf{G} \mathbf{u}_0(\mathbf{k}). \quad (4)$$

The \mathbf{W} operators in (4) can be defined for variable water velocity and rough sea, as well as for an arbitrary cable profile. Using (4), de-ghosting corresponds to solving for \mathbf{u}_0 , and requires the inversion of \mathbf{G} .

Information relating to the cable depth and water velocity are routinely acquired during a survey. A kurtosis-based approach can later be used during data processing to optimize the receiver depths when required (Grion et al. 2015). In the context of phase-shift de-ghosting, with a kurtosis approach equation (4) would be solved a number of times using a limited data portion and a series of trial receiver depths. The estimated depth for each receiver location would correspond to the highest kurtosis value. This approach is well suited for the estimation of slow-varying cable depth variations, because of the implicit spatial smoothness that this approach imposes on cable depth estimates.

Rough sea estimation

In situations when the rough sea has a visible impact on seismic data (Figure 1), seismic data itself can be used to estimate a sea-surface profile.

The sea-surface profile may be measured or estimated at each channel location, for example, by methods discussed in Kragh et al 2004), Hardwick et al. (2015) and King and Poole (2015). We confirm that in our experience it is possible to use the f - x - y spectrum of selected events as a ghost-primary interferogram (Figure 2), and infer a sea surface profile from the frequency of ghost notches.

Once the cable depth and events' arrival angles are properly taken into account, the ghost notches provide information on the ghost delay time. Depending on cable

Rough-sea estimation for phase-shift de-ghosting

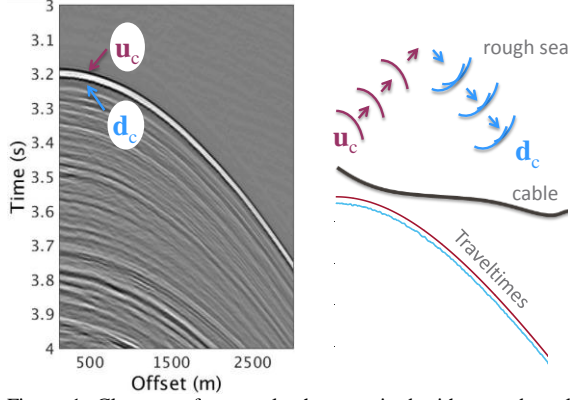


Figure 1: Close-up of a sample shot acquired with a moderately rough sea (2m SWH on observer logs). The down-going sea-bottom ghost reflection \mathbf{d}_c shows lateral coherency variations that are absent in the corresponding up-going.

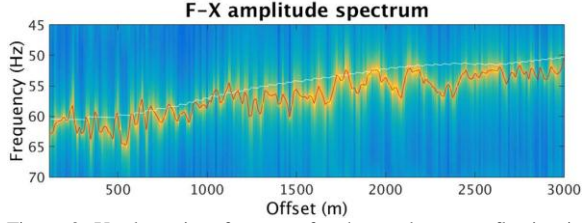


Figure 2: Up-down interferogram for the sea-bottom reflection in Figure 1. In the spectral colormap, yellow indicates the ghost notch. The white line is the predicted notch location for a calm sea and is used as a guide function for picking. The red line is the picking result.

depth and maximum frequency in the data, it is sometimes useful to jointly consider more than one order of ghost notches for this purpose. If a time-variant sea surface profile is required, rough-sea estimation and de-ghosting can take place in time windows.

A key aspect of the rough sea estimation process we propose is an iterative tomographic back-propagation of the estimated sea surface elevation. With deep, variable-depth cables and rough seas, the $[x,y]$ spatial location of a certain ghost delay-time picked from a spectrum is not identical to the $[x,y]$ spatial location of the sea-surface elevation that generated it, especially for shallow water surveys. Therefore, we proceed with an iterative approach where initially the sea surface is assumed to be flat. At the first iteration, a vertical update gives a first estimation of the rough sea surface. With subsequent iterations, ray-tracing from the variable-depth cable to the rough sea-surface and back allows for updates along the ray directions. This iterative process is repeated until the modelled ray-traced ghost delay times fit the delay times picked for the f - x data ghost notches with a given tolerance.

De-ghosting posterior covariance

Can variable-cable depths and rough-sea surfaces aid pre-migration de-ghosting? This question can be answered by a covariance study.

The formulation of de-ghosting as an inverse problem allows the calculation of *posterior* covariances based on assumptions on *prior* total and up-going pressure uncertainties. Assuming prior Gaussian uncertainties characterized by covariance matrices \mathbf{C}_{p_e} and $\mathbf{C}_{\mathbf{u}_0}$, the posterior covariance $\tilde{\mathbf{C}}_{\mathbf{u}_0}$ for the estimation of \mathbf{u}_0 is (Tarantola 2005, p. 36)

$$\tilde{\mathbf{C}}_{\mathbf{u}_0} = (\mathbf{G}^* \mathbf{C}_{p_e}^{-1} \mathbf{G} + \mathbf{C}_{\mathbf{u}_0}^{-1})^{-1}.$$

Similarly to Grion et al. (1998) and Davison et al. (2011), we use the posterior covariance as a tool to assess the effect of acquisition geometry on inversion result. Grion et al. (2016) calculated $\tilde{\mathbf{C}}_{\mathbf{u}_0}$ for a range of cable depth profiles and with a calm or rough sea-surface to assess the effect of notch diversity on pre-migration de-ghosting. This study is summarized below.

Figure 3 (top) considers a set of cable depth profiles and shows $\tilde{\mathbf{C}}_{\mathbf{u}_0}$ for the calm and rough sea cases in the 0-125Hz band. For each frequency, the square roots of the diagonal elements (standard deviations) of $\tilde{\mathbf{C}}_{\mathbf{u}_0}$ are normalized and displayed as a frequency-wavenumber map. The standard deviations are symmetric with respect to wavenumbers. For convenience, calm and rough sea values are displayed side by side for every cable profile.

The rough sea used for the calculations in Figure 3 is a Pierson-Moskowitz sea surface (see e.g. Clay and Medwin 1977) with 4m significant wave height. It can be noted that in the calm-sea case the perfectly flat cable presents large errors in correspondence to the receiver ghost notch, and that the variations in cable depth of other profiles smooths the de-ghosting errors. Maximum smoothing is achieved with the strongest cable depth variation. The presence of a rough sea-surface tends to equalize covariance differences for the various cable profiles.

For both rough seas and variable cable depths the covariance levels tend to become more uniform, a sign that any input white noise level will be less distorted in output. This is a desirable feature, as white noise can be reduced by stacking and other signal preserving random noise attenuation methods (e.g. Gaetani et al., 2016).

It is important to point out that variable-depth cables and rough seas help the de-ghosting process only if they are known with sufficient accuracy and if the de-ghosting

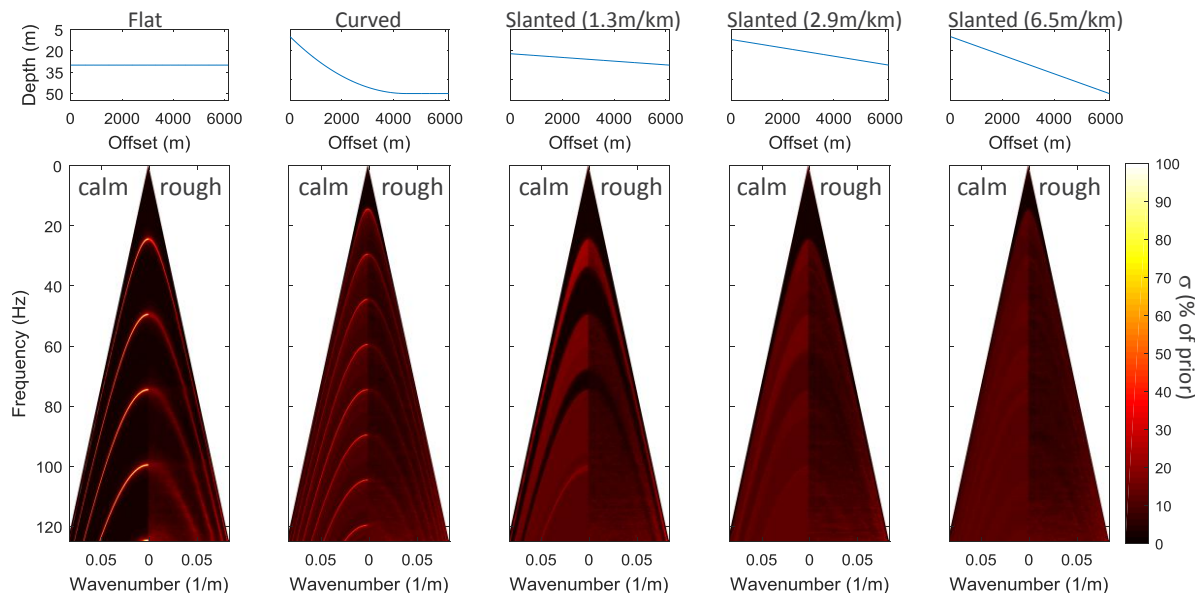


Figure 3: De-ghosting posterior standard deviation as a function of frequency and wavenumber. Dark colours indicate small errors; a value of 100 indicates unreliable de-ghosting.

algorithm can handle them precisely. If either of these conditions are not met, they act as additional sources of noise and artefacts.

De-ghosting example

We consider four sample shots from the Carnarvon survey acquired in deep water offshore NW Australia, with trace edits and swell noise attenuation applied as pre-processing. The observer logs mention rough seas with 2.0 m SWH during acquisition. Figure 4 (top) shows a close-up of the shots and their cable depth profiles. As noted in Figure 1, inspection of these close-ups shows that the receiver ghost presents a level of spatial variability not visible in the corresponding up-going events. Receiver depths cannot therefore be the cause of these variations. Figure 4 (bottom) shows a phase-shift de-ghosting attempt on this data, using a calm sea-surface. Ghost energy is attenuated, but visible artefacts appear in the de-ghosted result. A sea-surface reflectivity of -1 was used for this test. This calm sea result could be improved using the average frequency-dependent reflectivity for this rough sea situation. In other words, -1 is not the optimal sea surface reflectivity for de-ghosting rough sea data using a calm sea approximation. In our experience this would substantially reduce the artefacts, but not remove them completely.

Figure 5 shows the de-ghosting result obtained using a rough-sea surface estimated using the tomographic procedure outlined in this paper. It should be noted however, that because of the deep water setting the

estimation converged during the vertical update (i.e. after the first iteration of the tomographic procedure). The estimated sea surfaces are shown at the top of the figure. These de-ghosting results represent a significant improvement over those in Figure 4 (bottom) and were obtained using the same de-ghosting parameters, including a -1 reflectivity for the sea surface. In other words, differences between the de-ghosting results in Figure 4 and Figure 5 are only due to the inclusion of sea-surface roughness in the \mathbf{W} operators of equations (2) and (3).

Conclusions

The up-going wavefield recorded by an arbitrary cable profile and rough sea is estimated by solving a linear system of equations. The calculation of the posterior covariance associated with this system provides intuitive insights on the effect of acquisition geometry and sea-state on de-ghosting results. In particular, a depth-varying cable profile is desirable for de-ghosting purposes, but rough seas tend to reduce differences induced by cable depth profiles. Application of the discussed rough sea estimation and de-ghosting method to data acquired in 2.0m SWH rough seas and a slanted profile provides satisfactory results.

Acknowledgements

The Carnarvon data shown are courtesy of Dolphin Geophysical multi-client department. Data acquisition took place offshore Australia by Dolphin Geophysical and project partner TGS.

Rough-sea estimation for phase-shift de-ghosting

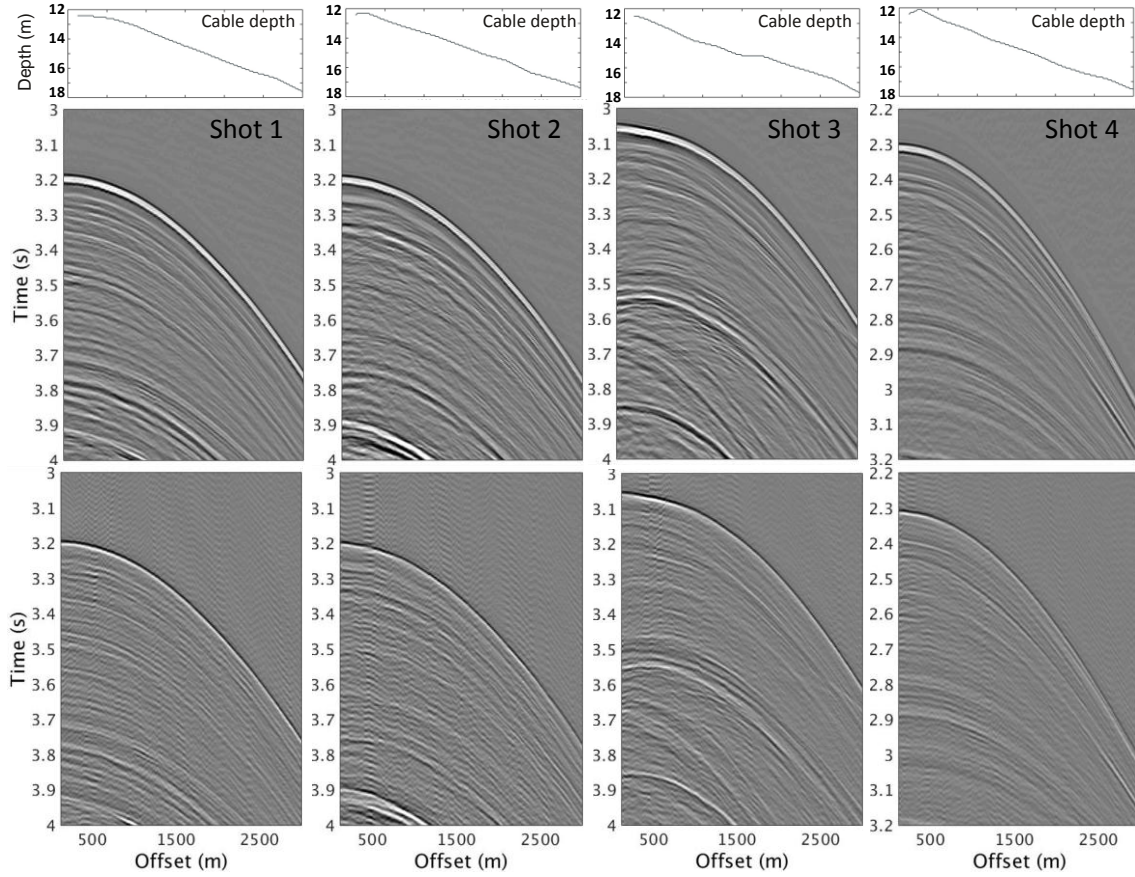


Figure 4: A set of four shots extracted from a line acquired using a slanted cable profile in the presence of a moderate rough sea (2m SWH), before (top) and after (bottom) phase-shift de-ghosting. In this de-ghosting example, the sea-surface is assumed to be flat.

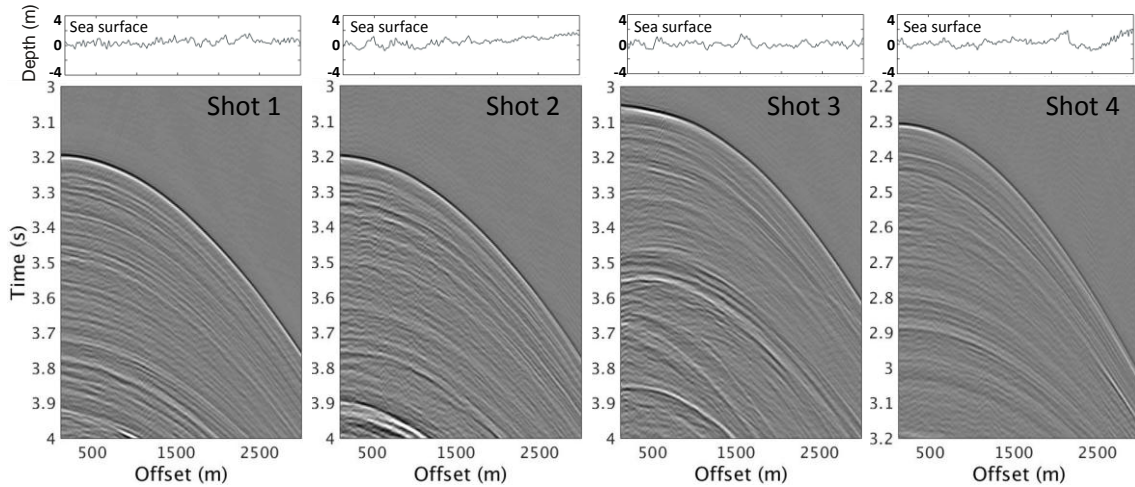


Figure 5: The four shots in Figure 4 after phase-shift de-ghosting using the rough sea-surface profiles shown.

Rough-sea estimation for phase-shift de-ghosting

References

Clay, C. S. and H. Medwin, 1977, *Acoustical oceanography: Principles and applications*: John Wiley & Sons.

Davison, C., Ratcliffe, A., Grion, S., Johnston, R., Duque, C., Neep, J. and M. Maharramov, 2011, Azimuthal velocity uncertainty: estimation and application: 81st Annual SEG Meeting, Expanded Abstracts, 264-268.

De Gaetani, C., Winters, S., Barnes, J. and S. Grion, 2016, Practical Aspects of Non Local Means Filtering of Seismic Data: 78th EAGE Conference, Extended Abstracts, Th STZ1 02.

Grion, S., Ruffo, P. and F. Rocca, 1998, Dispersion of 3D velocity estimators: 60th EAGE Conference, Extended Abstracts, 1-04.

Grion, S., Telling, R. and J. Barnes, 2015, De-ghosting by kurtosis maximization in practice: 85th SEG Meeting, Expanded Abstracts, 4605-4609.

Grion, S., Telling, R. and S. Holland, 2016, Phase shift de-ghosting, 78th EAGE Conference, Extended Abstracts, We SRS3 09.

Hardwick, A., Charron, P., Masoomzadeh, H., Aiyepoku, A., Cox, P. and S. Laha, 2015, Accounting for sea surface variation in deghosting – a novel approach applied to a 3D dataset offshore West Africa: 85th Annual SEG Meeting, Expanded Abstracts, 4615-4619.

King, S. and G. Poole, 2015, Hydrophone-only receiver deghosting using a variable sea surface datum: 85th Annual SEG Meeting, Expanded Abstracts, 4610-4614.

Kragh, E., Robertsson, J.O.A., Laws, R., Amundsen, L., Rosten, T., Davies, T., Zerouk, K. and A. Strudley, 2004, Rough-sea deghosting using wave heights derived from low-frequency pressure recordings – a case study: 74th Annual SEG Meeting Expanded Abstracts, 1309-1312.

Masoomzadeh H., N. Woodburn, and A. Hardwick, 2013, Broadband processing of linear streamer data: 83rd Annual SEG Meeting Expanded Abstracts, 4635-4639.

Poole, G., 2013, Pre-migration receiver de-ghosting and re-datuming for variable depth streamer data: 83rd Annual SEG Meeting, Expanded Abstracts, 4216-4220.

Riyanti, C.D., van Borselen, R.G., van den Berg, P.M. and J. T. Fokkema, 2008, Pressure wave-field deghosting for non-horizontal streamers: 78th Annual SEG Meeting, Expanded Abstracts, 2652-2656.

Tarantola, A., 2005, *Inverse problem theory*: SIAM.

Wang, P., S. Ray, C. Peng, Y. Li and G. Poole, 2013, Premigration deghosting for marine streamer data using a bootstrap approach in Tau-P domain: 83rd Annual SEG Meeting, Expanded Abstracts, 4221-4225.